Received: 25 September 2018 | Revised: 9 December 2018 | Accepted: 11 December 2018

DOI: 10.4218/etrij.2018-0532

SPECIAL ISSUE

WILEY ETRI Journal

Recent advances in metasurface hologram technologies

Gun-Yeal Lee | **Jangwoon Sung** | **Byoungho Lee**

School of Electrical and Computer Engineering, Seoul National University, Seoul, Rep. of Korea.

Correspondence
Byoungho Lee, School of Electrical and Computer Engineering, Seoul National University, Seoul, Rep. of Korea.
Email: byoungho@snu.ac.kr

Funding information
This work was supported by Basic Science Research Program through the National Research Foundation of Korea (NRF) funded by the Ministry of Science and ICT (2017R1A2B2006676).

Since Leith and Upatnieks demonstrated the first optical hologram in 1964, hologram technology has attracted a great deal of interest in a wide range of optical fields owing to its potential use in future optical applications such as holographic imaging and optical data storage. Although there have been considerable efforts to develop holographic technologies using conventional optics, critical issues still hinder future development. Recently, metasurfaces composed of artificially fabricated subwavelength structures have been considered as novel holographic devices that show an unprecedented ability to control electromagnetic waves. In this review, we outline the recent progress in metasurface holography. A general introduction to several types of metasurface holography categorized based on their physics and application is provided. Then, our personal perspective on the future of this field is discussed.

KEYWORDS
holography, meta-hologram, Metasurface, nanophotonics, spatial light modulation

1 | INTRODUCTION

Holography is an optical technology that records and reconstructs wavefronts of light analogously or digitally, and has exhibited potential for use in next-generation imaging technology with various applications such as three-dimensional holographic imaging and optical data storage [1–3]. To achieve holographic images, various holographic devices, including spatial light modulators and diffractive optical elements, have been explored, but their limited capabilities have hindered further development of holographic technology. In particular, existing holographic devices provide resolution of only a few microns in their reconstruction-process, in which a subwavelength-scale resolution is required to remove any other diffraction orders obstructing the reconstructed holographic images. Moreover, the current state-of-the-art holographic devices only provide either phase or amplitude modulation of light, while both are required to completely reconstruct wavefronts of light in holography.

A metasurface is a flat optical device composed of artificially fabricated subwavelength nanostructures, namely meta-atoms, with unique optical responses not found in nature [4–8]. Owing to its extraordinary light modulation ability, it can enhance or even implement optical phenomena that have not been previously observed in nature [9-14]. Thus, metasurfaces have been used to replace conventional bulk optics in a variety of optical applications. Recently, researchers in the field of metasurface have focused on wavefront engineering because of its ability to design optical responses in subwavelength regions [15–18]. It has been found that, by designing subwavelength nanoantenna morphologies in metasurfaces, a wide range of light-mater interactions can be obtained. In this context, an attractive metasurface application is metasurface holography [19–21]. In particular, numerous approaches have been proposed to implement novel holographic devices, and metasurfaces have been found to provide high-quality holographic reconstruction of light with spatial amplitude and phase information at a subwavelength resolution. As metasurface holograms have many advantages and features over conventional holograms, metasurface holography is expected to make holographic technology a promising application for everyday life.

In this review, we introduce the basic concepts and recent advances of metasurface holography. We organize

the contents into several categories as follows. First, we introduce representative metasurface principles for wavefront engineering, and discuss metasurface holograms with phase modulation. Then, metasurface holograms with complex-amplitude modulation that completely eliminate the chronic problems of traditional holography are introduced as a next step. Various wavelength-multiplexed metasurface holograms for full-color holography are also discussed. Next, we introduce the polarization multiplexing achieved by using meta-holograms in which different holographic images can be switched between each other by tuning the polarization states of the incident light. Then, active metasurface holograms, which can be electrically or chemically controlled, are discussed. Finally, our personal views on the future of metasurface holography are provided.

2 | BASIC PRINCIPLES OF METASURFACES

As holography is an optical technique for recording and reconstructing the wavefront of electromagnetic waves, an ability to record and reconstruct spatial amplitude or phase distribution is fundamentally required to materialize holographic devices. Therefore, studies on metasurface holography are related to developing amplitude or phase modulating structures with some additional functionalities. Various principles have been applied to develop metasurface holography. In this section, we summarize some of the most representative principles among the proposed physics in metasurface holography.

2.1 | Meta-atoms with plasmonic resonance

In the early stages of wavefront shaping metasurface development, the first proposed meta-atom fully controlling the phase of light from 0 to 2π was a V-shaped antenna [14]. The V-shaped antenna is composed of two identical gold nanorods with an arbitrary angle, in which the length of the nanorod and the angle between the two nanrods determine the transmission behavior through the meta-atom. There are two resonant modes in this plasmonic meta-atom, that is, symmetric and antisymmetric modes according to the induced current distribution, and the physics of the meta-atom is based on the hybridization of these two modes. As shown in Figure 1A, the symmetric mode is excited under linear polarization along the symmetry axis of the meta-atom, while the antisymmetric mode is excited under orthogonal polarization. Therefore, any other linear polarization other than the two aforementioned polarizations induces both resonant modes, leading to the hybridization of two resonant modes. As a result, there are two components in the scattered light from the meta-atom that contribute to the desired phase modulation: one is a co-polarized component with normal transmission and the other one is a cross-polarized component with anomalous transmission. Here, co- or cross-polarization mean identical or mutually orthogonal polarizations, respectively, compared with the polarization of input light. Yu et al have shown that several combinations of the lengths and angles of the arms of V-shaped antenna successfully provide full-phase modulation from 0 to 2π as shown in Figure 1B [14]. Although this first attempt was impressive in terms of wavefront manipulation, the meta-atom is limited to plasmonic materials owing to its resonant origin; therefore, its efficiency and bandwidth are quite limited. Furthermore, this method is based on using cross-polarized components rather than incident polarized components. This complicated mechanism hinders its further use in optical applications.

2.2 | Pancharatnam-Berry phase meta-atom

Phase or amplitude modulation via the aforementioned methods is based on a change in antenna geometry, so highly accurate fabrication and narrow bandwidths are needed. Rotation of rectangular nanorods with dielectric or plasmonic materials provides full-phase modulations with broadband characteristics in circular polarization states as shown in Figure 1C [22]. This is based on the spin-rotation coupling of light, which is generally called the Pancharatnam-Berry phase (PB phase) or geometric phase. The theory of the PB phase can be derived from considering the optical response of an arbitrarily anisotropic nanorod. An anisotropic nanorod can be represented by a Jones matrix **J** within the coordinates consisting of a longer and shorter optical axis as follows,

$$\mathbf{J} = \begin{pmatrix} t_l & 0 \\ 0 & t_s \end{pmatrix}, \tag{1}$$

where t_l and t_s are the complex coefficients for longer and shorter optical axes, respectively. Using the Jones matrix, a nanorod with an orientation angle of θ can be calculated using a rotation matrix $\mathbf{R}(\theta)$, resulting in $\mathbf{T} = \mathbf{R}(-\theta)\mathbf{J}\mathbf{R}(\theta)$. Now, in the case of a circularly polarized incidence with a handedness of σ (where $\sigma = 1$ or -1 for right or left circular polarization, respectively), the complex transmittance from the nanorod can be calculated using the Jones matrix **T** as follows:

$$E_t = \mathbf{T}|\sigma\rangle = \frac{t_l + t_s}{2}|\sigma\rangle + \frac{t_l - t_s}{2}e^{\mp j2\sigma\theta}|-\sigma\rangle, \tag{2}$$

where the Jones vectors for circular polarization is represented as $|\pm\sigma\rangle = [1 \quad \pm j\sigma]^T/\sqrt{2}$. As shown in the right side of (2), the complex transmittance for circularly polarized incidence is composed of two orthogonal components with their own complex amplitudes, while the phase delay, which is related to the orientation angle θ, exists only in

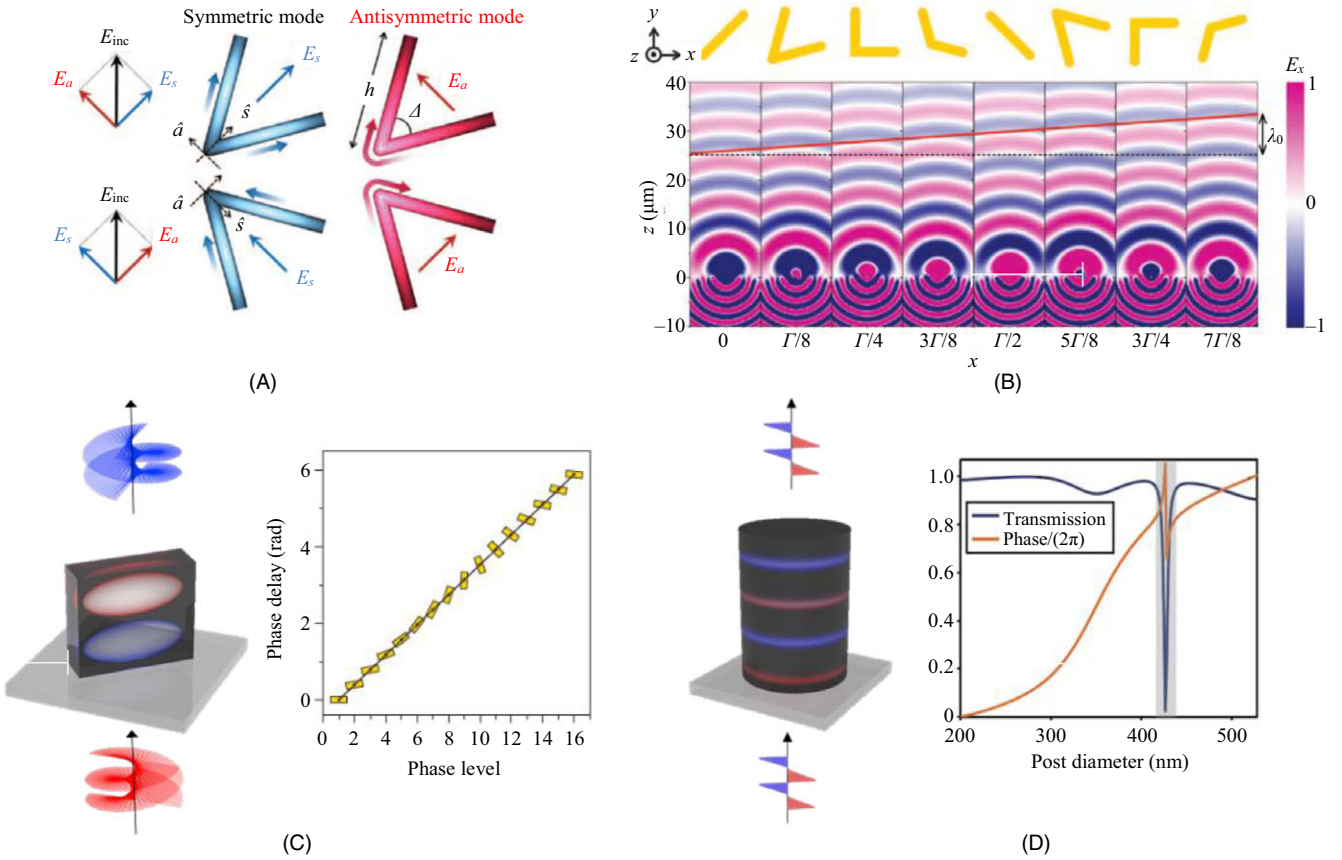

FIGURE 1 Meta-atoms for phase modulation. (A) Schematic illustration of the physical mechanism of V-shaped antenna. Superposition of the symmetric and antisymmetric modes is designed by parametric changes of the V-shaped antenna, resulting in realization of full-phase modulation of transmitted light [14]. (B) Phase gradient for beam deflection can be realized by utilizing these V-shaped antennas [14]. Γ represents a period of V-shaped antenna array, and X and Z represent spatial coordinates. (C) Schematic of a Pancharatnam-Berry phase meta-atom using nanorods under circularly polarized incidence, where the phase delay of the scattered light is determined by the orientation of nanorods [28]. (D) Schematic of a dielectric waveguide post where the phase delay is controlled by change of the post diameter [23]

the cross-polarized component, as shown in Figure 1C. As the PB phase depends only on the orientation angle of the nanorod, other factors like wavelength do not affect the PB phase; thus it has a broadband nature.

2.3 | Dielectric meta-atom with propagation phase

All-dielectric metasurfaces have a clear advantage in terms of efficiency owing to the lower absorption coefficients of dielectric materials than metals in the visible or near infrared region [7,8]. A typical shape of a meta-atom is a cylindrical post. From the viewpoint of the refractive index, there are two main principles for determining the optical behavior of the dielectric meta-atoms. For example, a cylindrical meta-atom with a low-index dielectric can be regarded as a kind of dielectric waveguide. Therefore, the phase information can be modulated by the effective refractive index determined by parameters such as the height or size of the post [23]. Figure 1D shows the schematic of a low-dielectric post when the linearly polarized light is incident normally to the post. The graph on the right panel shows simulation results representing the amplitude and phase of the transmitted light in terms of post diameter, and we can see that the phase can be fully controlled from 0 to 2π, while the amplitude is almost constant. Some fluctuations in the amplitude and phase of the colored areas occur due to resonance, which should be avoided to design a metasurface, but do not interfere with the arbitrary design of the phase profile.

On the other hand, high-index dielectrics, like silicon, in the visible region, have a relatively strong resonance, and the geometry of the meta-atom determines the resonance modes or intensity. For example, electric dipole modes and magnetic dipole modes are dominant in general cases, while other higher modes also exist. Recently, it was reported that the carefully designed silicon nanodisk has almost equal amounts of electric and magnetic dipole

modes, resulting in a high transmission metasurface without reflection. This is due to the symmetry characteristics of the resonance modes, where the electric dipoles induce symmetric scattering, but the magnetic dipoles induce asymmetric scattering. Their sum results in constructive or destructive interference in transmission or reflection, respectively. Such metasurfaces are called Huygens' metasurfaces and recently have been applied in designing high efficient metasurfaces in the visible spectrum [24,25].

3 | METASURFACE HOLOGRAPHY

Based on the concepts introduced in the previous section, as well as the use of additional physics, various metasurface holograms have been proposed over the last few years. In this section, we outline types of metasurface holograms, including transmissive or reflective meta-holograms, complex-modulated meta-holograms, multicolor meta-holograms, multiplexed meta-holograms, and active meta-holograms.

3.1 | Phase-only holograms

The first stage of metasurface holography involves showing phase-only holograms with subwavelength phase modulations. Compared to conventional holography, metasurface holograms possess subwavelength pixel resolution, which is important in optical holography; the size of pixel determines not only the image resolution, but also the viewing angle of the reconstructed holograms, which is crucial in three-dimensional holography. On the other hand, micron-scale resolutions in conventional holography make the holographic images have narrow viewing angles of about a few degrees. Therefore, the first demonstration of metasurface holography with subwavelength resolution was impressive and solved the chronic bottlenecks in conventional holography.

A V-shaped plasmonic antenna was employed to realize metasurface holography with full-phase modulation in linear polarization states, while the previous works based on the V-shaped antenna only focused on beam deflections [14,26]. The study sufficiently showed powerful performance owing to the subwavelength resolution of the metasurface holography. In addition, broadband three-dimensional holography based on the PB phase has been suggested for successfully reconstruction of three-dimensional holographic images [27]. This result demonstrates the potential of three-dimensional broadband metasurface holography, and this was an important early attempt for numerous further studies in the future.

Although the aforementioned attempts successfully showed metasurface holography with full- and subwavelength phase modulation, efficiency was low owing to metallic loss in the visible spectrum. In order to overcome the efficiency issue, pioneering works have been suggested. Zheng et al have shown that a multilayered design of a reflective metasurface dramatically improves the efficiency of the surface [28]. The proposed metasurface is composed of metal-insulator-metal (MIM) layers and a top metal layer that consists of gold nanorod arrays to describe phase profiles according to the PB phase. This scheme generates multiple reflections in the internal layer and then enhances the reflection efficiency. Furthermore, as it is a highly accurate design that enables matching of the half-wave plate condition, the conversion efficiency between the modulated and incident light is optimized. As a result, the phase holograms achieve a diffraction efficiency over 50% in a broad bandwidth over 400 nm, where the maximum efficiency is over 80% at a wavelength of 825 nm, as shown in Figure 2D. Compared to the efficiencies obtained in previous studies, an 80% efficiency was remarkable, and this multilayer approach has been applied in the design of various reflective metasurfaces.

For transmission, all-dielectric metasurfaces have come to the fore because dielectrics experience much less loss than metals. Figure 2E shows a Huygens' metasurface hologram that has near unity efficiency with phase modulation [25]. More recently, other methods for obtaining a much higher efficiency have been suggested. Several metal dioxides or nitrides like TiO_2, SiN_x, and GaN typically have almost zero absorption in the visible region, even though they have high refractive indices of about 2–3 [29–31]. For future metasurface holography, these materials would play an important role in the design of optical metasurfaces, although issues like the fabrication difficulty of the materials remain.

3.2 | Complex-amplitude holograms

Most of the existing holograms and metasurface holograms are based on phase-only methods that describe the holographic images as shown in the previous section. Although metasurface holography with phase modulation provides higher resolution compared to conventional holography, a critical problem regarding image quality still remains. In theory, holography essentially requires both amplitude and phase information to ultimately reconstruct the desired electromagnetic waves. However, the current spatial light modulators and many holographic metasurfaces cannot provide both amplitude and phase modulation. This is because the operating mechanisms for controlling the amplitude or phase of a conventional device and metasurface fundamentally interfere with each other, which is problematic for independent and complete control of both amplitude and phase. Therefore, phase- or amplitude-only holograms exhibit critical noise or destructed wavefronts in the image plane owing to a lack of light information.

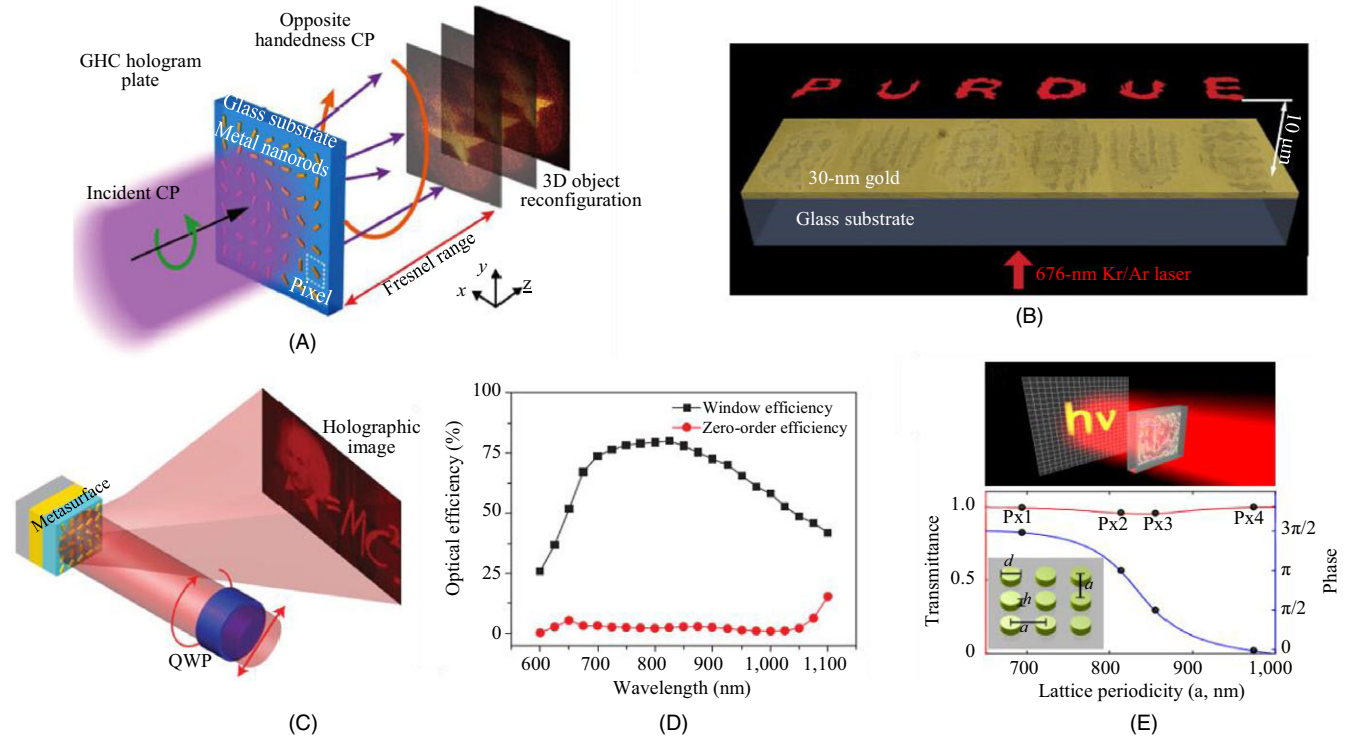

FIGURE 2 Meta-holograms with phase modulation. (A, B) Transmission-type metasurfaces for three-dimensional on-axis holography composed of (A) gold nanorods with PB phase [27] and (B) V-shaped gold apertures [26]. It is notable that Ref. 26 also provides two-level amplitude modulation as well as eight-level phase modulations. (C) Reflection-type off-axis metasurface hologram composed of gold nanorods with a metal-insulator-metal layer [28]. By virtue of the metal-insulator-metal layer, the hologram has a high efficiency of ~80% and a broad bandwidth. (E) Huygens' metasurface hologram composed of silicon nanodisks showing a high efficiency in transmission mode [25]

In the metasurface field, there have been some attempts to implement full complex-amplitude modulation [26,32–34]. Ni et al have shown that V-shaped antennas with blank pixels can produce two-level amplitude and eight-level phase modulation, where a blank pixel means zero amplitude at that position [26]. A comparison of several cases reveals that a larger amplitude and more phase levels are needed to reconstruct sharper images (Figure 3A). Even though the proposed method cannot provide higher amplitude levels, it was a significant attempt to show the importance of complex-amplitude modulation.

To increase amplitude levels, a C-shaped antenna for the terahertz region was suggested as shown in Figure 3B. Like the V-shaped antenna, the C-shaped antenna also has two resonant modes, that is, the symmetric and antisymmetric modes, but the authors adopted this mechanism to fully control both the amplitude and phase profiles. Then, the orientation angle and open angle of the C-shaped antenna successfully achieve simultaneous control of both amplitude and phase, but this scheme was limited to the terahertz region [32].

In the visible spectrum, recent studies have shown that an X-shaped meta-atom provides independent, continuous, and broadband modulation of both amplitude and phase information within a subwavelength scale. The X-shaped meta-atom possesses two independent modes for the PB phase, which can be controlled by the orientation angles of the two arms of the X-shaped structure so that the arbitrary superposition of the modes results in an arbitrary complex value as shown in Figure 3D. This full and broadband complex-amplitude modulation successfully provides vivid complex-amplitude modulated holograms without any noise in the entire visible region, as shown in Figure 3E. Compared to the phase-only holograms, this hologram achieves a signal-to-noise ratio (SNR) of 211, which is much higher than the SNR of 50 for phase-only metasurface holography [34]. Another advantage of complete complex-amplitude modulation is elimination of the limited zone in designing computer generated holograms. For the holograms with phase-only modulation, the Fraunhofer condition should be considered to fully reconstruct the recorded information owing to a lack of amplitude information. This means that some distances from the wavefront plane (ie, the metasurface plane) should be provided, as the allowed space for holography is limited. However, complex-amplitude modulation enables the holography to transcend the Fraunhofer condition so that even images can be reconstructed just above the metasurface plane, as shown in "S" images represented in Figure 3E [34].

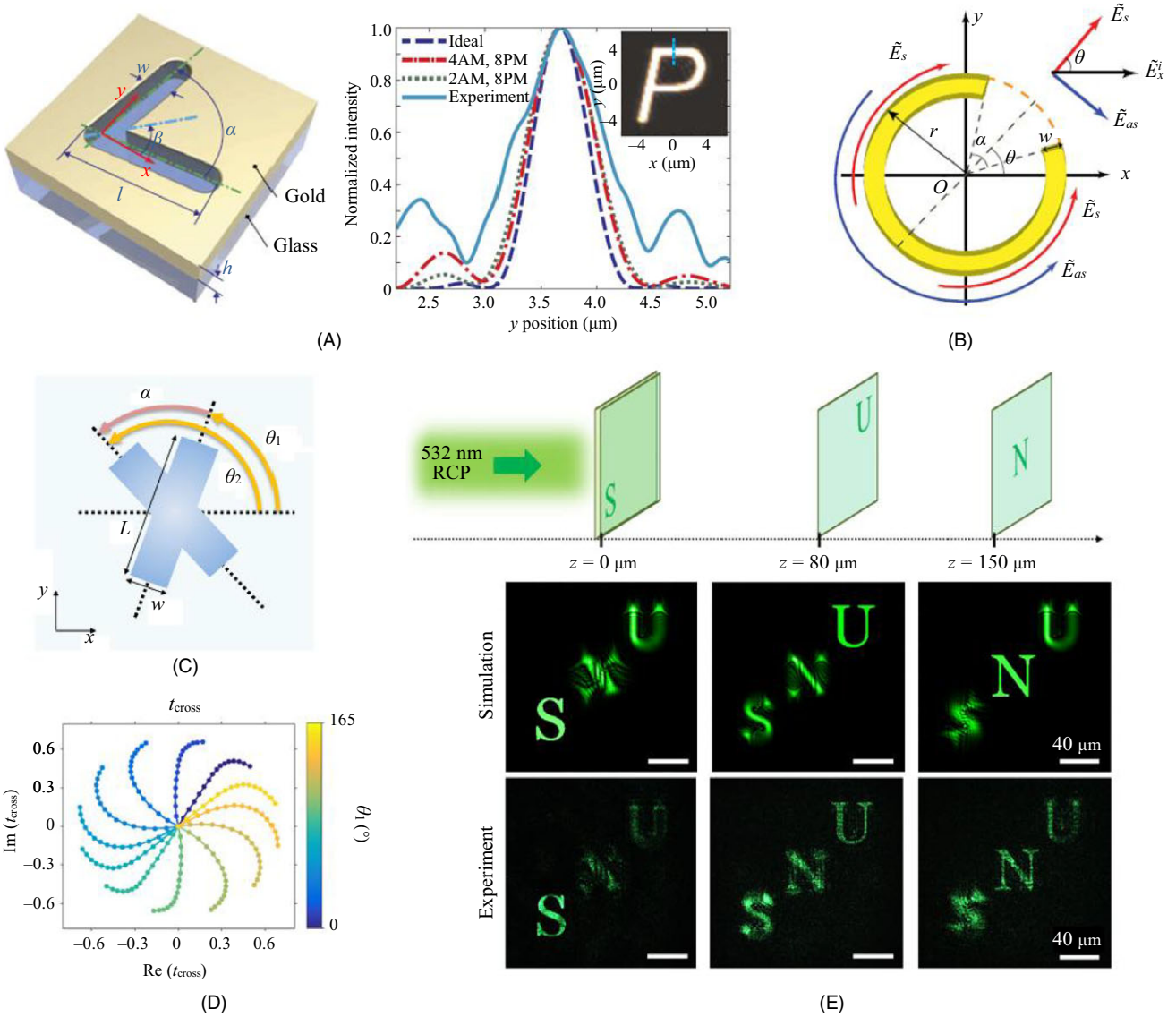

FIGURE 3 Complex-amplitude meta-holograms. (A) V-shaped gold nanoapertures for full-phase modulation (left); utilizing the V-shaped apertures, meta-holograms with two-level amplitude modulation and eight-level phase modulation is realized, showing improved image quality compared to the results with lower level modulation (right) [26]. (B) C-shaped aperture for full complex-amplitude modulation in terahertz spectrum [32]. (C) X-shaped dielectric meta-atom for full complex-amplitude modulation in the visible spectrum [34]. (D) Simulation results of complex transmittances from the X-shaped meta-atom represented in complex domain. t_{cross} means a transmission coefficient for cross-polarized component. (E) Holographic images with full and continuous complex-amplitude modulation by using the X-shaped meta-atoms

3.3 | Multicolor holograms

Although the PB phase provides broadband operation of the metasurfaces, full-color holograms require a more complicated strategy, such as wavelength-dependent phase control. This is also related to implementing achromatic optics in which different wavelengths require different wavefronts to equally act; however, this implementation is very challenging. Therefore, researchers studying full-color holograms started by employing indirect strategies. Wang et al have suggested a macro pixel composed of three different plasmonic nanorods [35]. Each of the nanorods has a different spectrum, and its resonance is specified for the target wavelength. Therefore, like a general display panel, the metasurface consists of spatially multiplexed pixels for providing multicolor holography, as shown in Figure 4A.

Another method for achieving multicolor holography is using an off-axis strategy. Figure 4B and C represent two metasurface holograms that are based on the off-axis strategy. Figure 4B shows a plasmonic metasurface consisting of nanoslits based on the PB phase [36]. For multicolor holography, a phase hologram that is composed of multiple

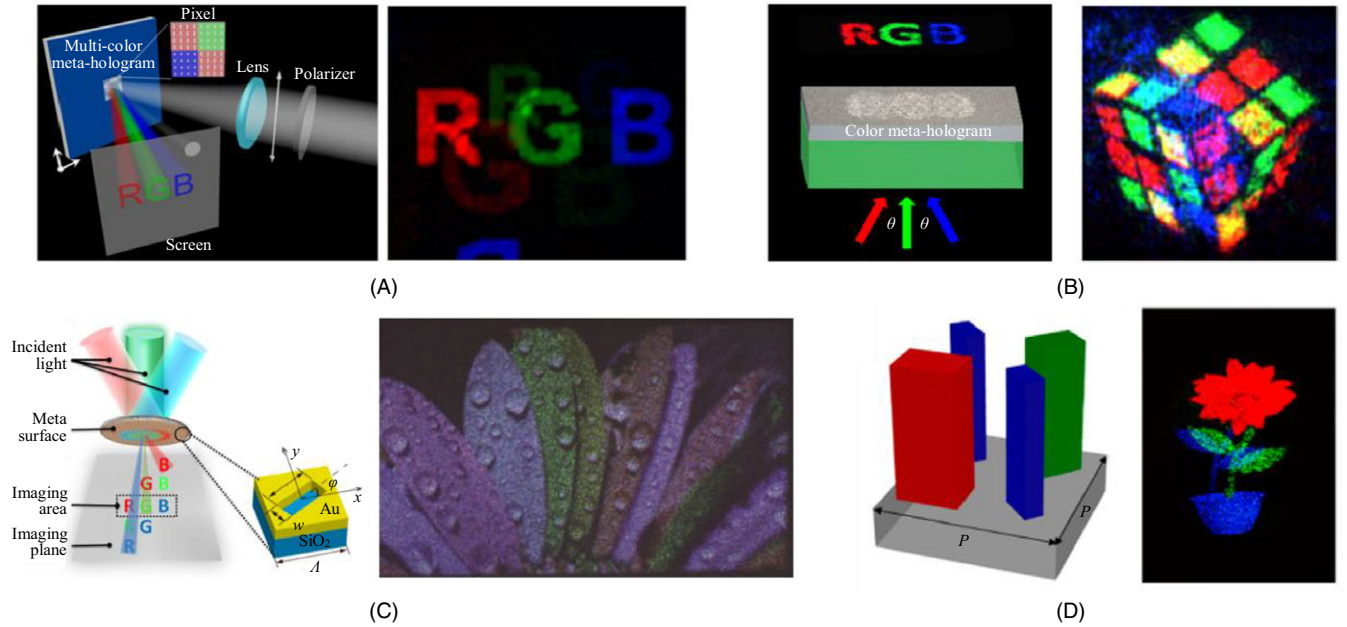

FIGURE 4 Multicolor metasurface holograms. (A) Reflection-type multicolor metasurface hologram composed of the aluminum nanorods [35]. Four kinds of nanorods are employed to construct a super-pixel for multicolor imaging, and the measured image is represented in right panel. (B) Schematic illustration (left) and experimental results (right) of the plasmonic metasurface composed of the nanoslit arrays, which utilizes the off-axis strategy with oblique incidences of three different wavelengths [36]. (C) Schematic illustration (left) and experimental results (right) of the plasmonic metasurfaces [37]. Compared to the results shown in (D), this metasurface hologram utilizes the characteristics of Fourier domain and seven colors to provide more vivid full-color images. (B) Multicolor dielectric metasurface hologram composed of multiplexed silicon nanorods (left) and experimental result [38]. Varying orientations and sizes of the nanorods determine the phase profiles and resonant frequencies, respectively, and combining three kinds of the nanorods in a subwavelength pixel provides high resolution multicolor images

images in which each image has a different wave vector component is designed. Then, three wavelengths with three different incident angles are applied to reconstruct the full-color hologram. It is worth noting that different incident angles move unwanted images at other wavelengths out of the measured area. In this way, only the target holographic images with target wavelengths are present in the image plane, while other unwanted images remain outside the measured area. Similarly, for Fourier domain imaging, oblique incidence induces a tangential component of the *k*-vector onto the metasurface plane, resulting in lateral shifts of the holographic images along with the tangential component of the *k*-vector. Figure 4C shows the schematics and results of a metasurface based on this scheme, and more complicated arrangements of seven wavelengths with their own incident angles realize full-color images [37]. These methods simply provide multicolor images with unwanted crosstalk, which should be solved for further development.

One can also design a wavelength-sensitive meta-atom that modulates the phase of light only at a specific wavelength and does not operate at other wavelengths. Using this idea, multicolor metasurface holograms with subcolor pixels have been developed in the subwavelength scale. As shown in Figure 4D, Huang et al designed a subwavelength super-pixel composed of four nanorods based on the PB phase [38]. The colors of the different nanorods in the figure represent their resonance wavelengths, which have narrow bandwidths, and the experimentally measured image shows the multicolor operation. Although the green and blue colors have some crosstalk, there are no other unwanted images compared to the other multicolor metasurface holograms. These attempts show the feasibility and possibility of full-color meta-holograms, but reducing noise from fabrication tolerances or pixel size remains a problem that must be solved in the future.

3.4 | Multiplexed holograms

To increase the degree of freedom of metasurface holograms, some kinds of metasurfaces have been proposed. One of the most popular methods for multiplexing is using polarization states of incident light, that is, the metasurface reconstructs different holographic images according to the input polarizations.

The most popular method for polarization multiplexing is utilizing the anisotropy of meta-atoms. For example, a rectangular metallic nanorod has higher scattering efficiency when the polarization of incident light is parallel than when it is vertical to the longer axis. Using this property, one can encode two different holographic images on

metasurfaces composed of parallel, perpendicular, and crossed nanorods as shown in Figure 5A [39]. The experimentally measured images show good agreement with the principal image, where the 45° polarization state induces both holographic images, but only four-level phase modulation could be possible in this scheme. Arbabi et al have suggested a new kind of anisotropic dielectric metasurface that provides arbitrary phase profiles for two orthogonal polarizations [40]. The proposed structure consists of silicon elliptical posts, where two ellipse diameters and orientation angles determine the two phase profiles of two orthogonal polarizations. This direct method for implementing polarization-multiplexed metasurfaces has a clear advantage in the reconstruction of the desired wavefronts

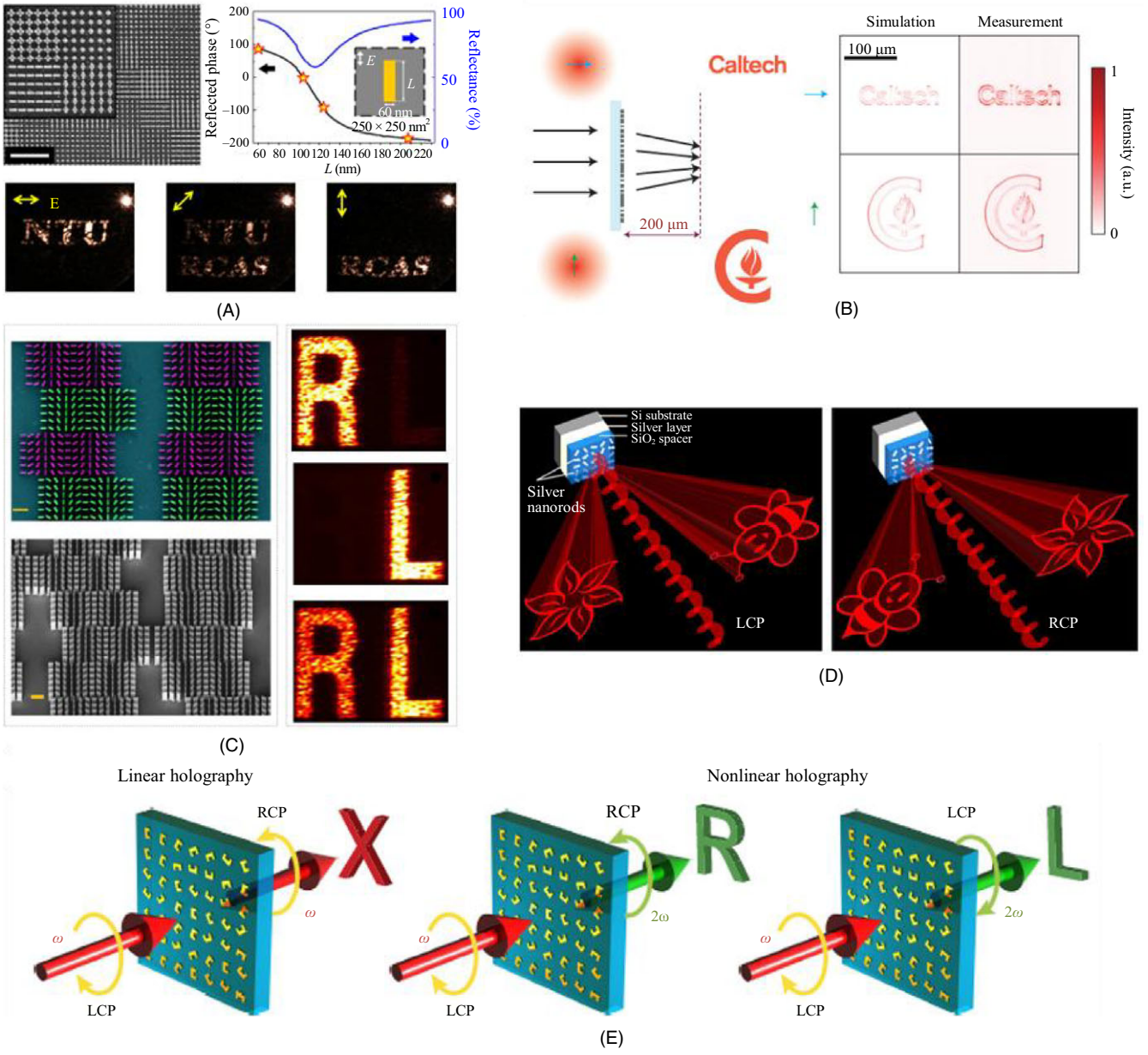

FIGURE 5 Polarization multiplexed holograms. (A) Polarization-multiplexed plasmonic metasurface holograms with four-level phase modulation by using asymmetric nanorods [39]. (B) Elliptical silicon posts possessing two independent phase information with respect to the longer and shorter axes, providing two independent holographic images for different linear polarizations [40]. (C, D) Spin-dependent metasurface holograms for circularly polarized states, showing different holographic images with respect to the incident handedness. (C) Dielectric nanorods implementing a super-pixel switching of the scattering direction according to the handedness of incident light [41]. (D) Alternately arranged nanorod arrays produce dual holographic images in Fourier domain where they are interchanged with each other according to the incident handedness. (E) Nonlinear plasmonic metasurface composed of C-shaped gold antenna, showing spin- and wavelength-dependent holographic imaging [42]

without any noise or crosstalk. More recently, this method has been further developed and advanced, as it generalizes the phase delay effects of anisotropic meta-atoms. By applying more generalization, Mueller et al have shown that the arbitrary two orthogonal polarizations can be set as a basis for the multiplexing process [41], which improves the utility of this multiplexing method for future development.

Circularly polarized light with two handedness can also be used for polarization multiplexing. For example, a nanodisk array with PB phase gradients can deflect the incident light to the right or left directions with respect to the incident handedness [42], and helicity-dependent metasurface holograms can be realized by arranging the super-pixel arrays. On the other hand, typical PB phase plasmonic metasurfaces can also be designed as helicity-dependent metasurface holograms, as represented in Figure 5D [43]. If the two different images are at different positions in the Fourier domain, the reversal of the incident handedness will switch them according to the center symmetry. This is due to the sign reversal of the PB phase, and this scheme can switch the reconstructed images to a specific viewpoint. Therefore, the PB phase method for multiplexing cannot record arbitrarily two different wavefronts, and it only provides the conjugate differences by the reversal of the input polarization. That means this method could not be applied for other cases requiring arbitrary wavefronts. On the other hand, as the method proposed by Arbabi et al could provide two arbitrary wavefronts, it can be applied for any kind of optical function as well as the multiplexing holographic images. However, PB phase methods have broad bandwidths, while the elliptical post properly operates only at a target wavelength.

Other methods for increasing the degree of freedom have been reported. For example, expansion of the PB phase method to the nonlinear regime yields an additional degree of freedom. As the PB phase effect is different in linear and nonlinear regimes, it can be used to realize second harmonic generation and wavelength- and spin-dependent metasurface holograms [44]. As shown in Figure 5E, the metasurface hologram that is multiplexed according to the fundamental or second harmonic frequency and also depends on the spin dependency is implemented. Other nonlinear metasurfaces that could be promising strategies to design metasurface holograms in the future have also been reported.

3.5 | Active meta-holograms

For practical usage of holographic display to be achieved, dynamic control of metasurface holograms is vital. Most of the metasurface holograms are static, and some of them just have several states. However, the limits of current fabrication technology make it challenging to materialize a number of nanoscale electrodes or other local controllers in a single metasurface. Nevertheless, a few studies on active metasurface holography have been reported recently.

A gigahertz metasurface composed of electrically controllable meta-atoms has been suggested [45]. The proposed structure is adopted in the electrode and changes the optical response according to the applied current. Although the metasurface is designed for much longer wavelengths than those in the optical region, this early attempt to invent an electrically tunable metasurface is an important example in this field.

There has been great interest in phase change materials whose optical response in the visible region can be varied. One of the most notable materials is $Ge_2Sb_2Te_5$ (GST), which has both metallic and dielectric states, and can be forced to switch from one state to another by electric or thermal signals. A few studies have been reported on the use of GST as a metasurface, including as a reconfigurable GST metasurface [46–48]. For metasurface holography, Lee et al suggested metasurface holograms based on GST in the visible spectrum while the optical response of GST is controlled by the electric signal as represented in Figure 6B [46]. A multilayered structure composed of GST and electrodes was designed, and experimental demonstrations for recording and reconstructing GST metasurface holograms with pixel sizes of 1 μm were successfully achieved. Furthermore, the feasibility for realizing a metasurface with a built-in electrode was also experimentally demonstrated, showing the future potential of GST for metasurface holography.

Furthermore, metasurface holograms can be dynamically controlled by using chemical reactions. Li et al showed that metal nanorods and a chemical reaction can be used to implement a dynamic hologram without big sacrifices in factors like pixel size and fabrication challenge [49]. The proposed metasurface consists of nanorods with various metals like magnesium, gold, and palladium. As each of the materials has a different chemical sensitivity to oxygen or helium gas, they can be used to design chemically controllable metasurface holograms that are also reconfigurable. This new approach to dynamic metasurface holograms provides a new possibility in this field.

4 | PERSPECTIVES IN METASURFACE HOLOGRAPHY

As we discussed in the previous section, the current meta-holograms can provide high-performances with multifunctionality in the passive manner. For ultimate holographic display, however, dynamic control of the hologram is essentially required. Hence, we believe that active control

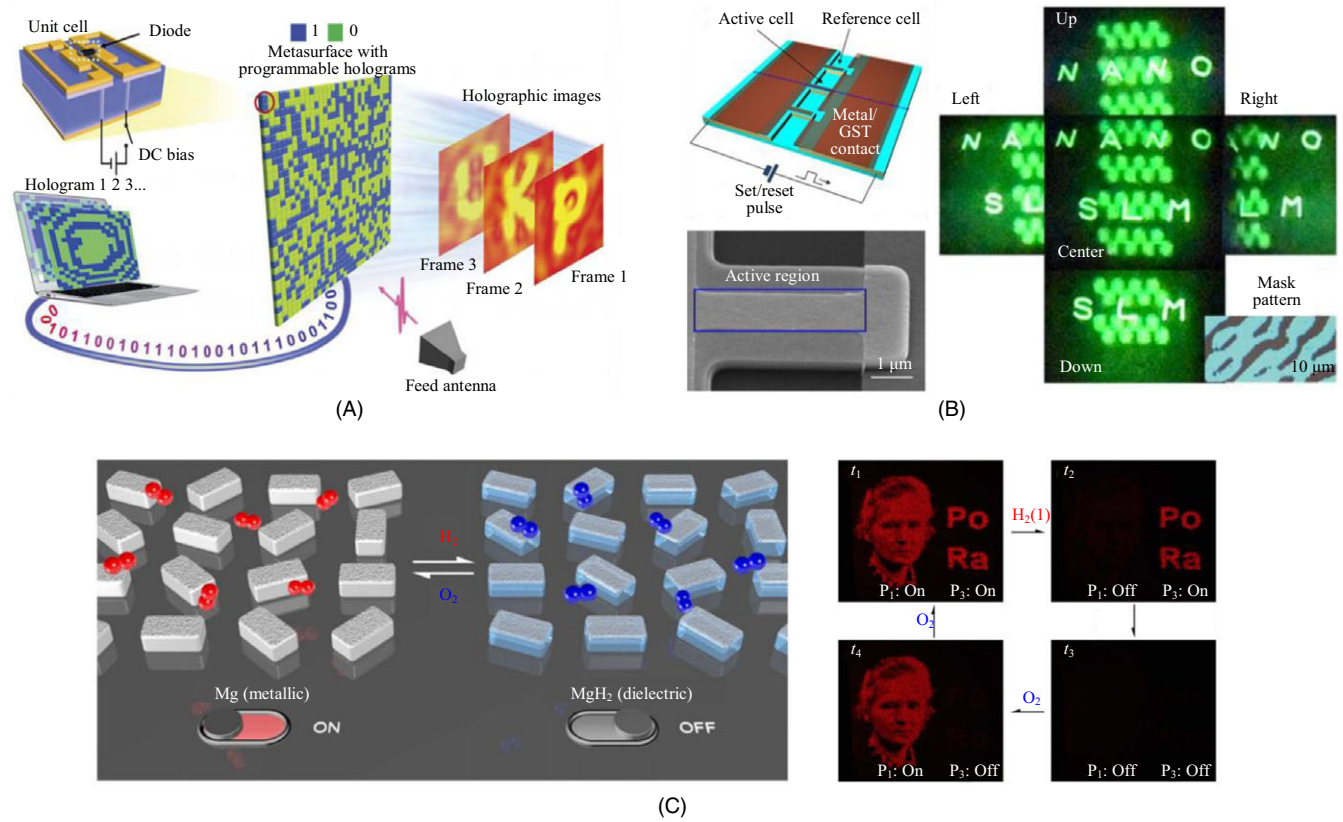

FIGURE 6 Active metasurface holograms. (A) Electrically tunable metasurface hologram with binary modulation in gigahertz region [45]. (B) Metasurface holograms based on Ge2Sb2Te5 (GST) in the visible region while the optical response of GST is controlled by the electric signal [46]. (C) Chemically tunable metasurface holograms composed of various metal nanorods [49]. Oxygen or helium gas induces chemical changes of the metal nanorods, resulting in switching reconstructed holographic images

TABLE 1 Summary of various metasurface holograms in terms of features, benefits, and remaining challenges

	Phase-only holograms			**Multifunctional holograms**		
	Reflection-type	**Transmission-type**	**Complex-amplitude holograms**	**Multicolored holograms**	**Multiplexed holograms**	**Active holograms**
Features	Meta-holograms with spatial phase modulation		Meta-holograms with both amplitude and phase modulation	Multicolored holograms within a single metasurface	Switchable meta-holograms with few degrees of freedom	Reconfigurable holograms via several methods including electric or chemical method
Benefits	High efficiency with broadband property	High efficiency in the visible spectrum	Perfectly reconstructed information, leading to vivid 3D holography	Multicolored images	Expanded degrees of freedom	Dynamic holographic imaging in real time
Challenges	High thermal loss and low efficiency in the visible spectrum	Hard fabrication of low-loss dielectrics	Relatively complicated mechanism, hindering scalability for active devices	Low image quality due to crosstalk, Low efficiency	Limited number of switchable images	Modulation time, modulation level, fabrication issues

of the metasurface is one of the most important goals in this field. Although some studies on active modulation have been reported in the last few years, as we have discussed in previous sections, their degrees of freedom have been limited, and continuous tunability with real time modulation is currently impossible; yet, it is required if practical metasurface holographic display are to be developed. We believe that these issues will be solved in the future by the development of nanofabrication technology and metasurface technology.

The use of holographic metasurfaces as optical components in current optical devices would be a great way to take advantages of metasurface holography. For example, the holographic display requires not only a spatial phase modulator but also a number of other optical elements such as lenses, mirrors, beam splitters, and diffusers. It is clear that metasurface optics can enhance the performance and compactness of current optical components. Moreover, other optical devices including microscopes, light field cameras, and virtual/augmented reality displays also need advanced optics, like metasurface optics, to improve their performances. Hence, we believe that the study of the application of current metasurface holograms in a variety of applications is as important as the development of metasurface holography itself.

In this context, very recent studies on metasurface optics have reported many promising applications besides holography. For example, a metasurface lens called a metalens has attracted great interest because it has clear advantages such as better performance and compactness compared to conventional refractive lenses [29–31,50,51]. It is notable that the metalens is very close to the metasurface holography while the metalens is a kind of holographic optical device designed to have a phase profile of a lens. Many remarkable studies on the application of metalens to various devices, such as microscopes [52], compact camera [53], spectrometer [54], endoscope [55], cryptography [56], and augmented reality displays [57], have been recently reported. Owing to the promising potential of metasurface optics, a variety of future applications that either improve current optical systems or provide a new kind of optical system will be proposed.

5 | CONCLUSION

In this review, we introduce the physical mechanism and concept of wavefront engineering metasurfaces. We then introduce various types of metasurface holograms such as complex-amplitude holograms, multicolor holograms, polarization-multiplexed holograms, and active holograms, as summarized in Table 1. Physical analysis and experiments reveal the excellent performance and versatile functionality of metasurface holography. We also discuss our perspective on this area. To conclude, the field of metasurface holography has enjoyed rapid development and rapid progress. We believe that metasurface holography will become more important in the field of holography because of its clear advantages when compared to traditional holography cannot be compromised. Furthermore, all the other photonics related to wavefront engineering will continue to require the development of metasurface holography, and advances in metasurface holography will also lead to advances in other kinds of photonic research. The field of metasurface holography is still vivid and prosperous, with new concepts and innovations in future applications.

ACKNOWLEDGMENTS

This work was supported by the Basic Science Research Program through the National Research Foundation of Korea (NRF) funded by the Ministry of Science and ICT (2017R1A2B2006676).

ORCID

Byoungho Lee https://orcid.org/0000-0002-0477-9539

REFERENCES

1. P.-A. Blanche et al., *Holographic three-dimensional telepresence using large-area photorefractive polymer*, Nature **468** (2010), 80–83.
2. J. Geng, *Three-dimensional display technologies*, Adv. Opt. Photon. **5** (2013), no. 4, 456–535.
3. B. Lee, *Three-dimensional displays, past and present*, Phys. Today **66** (2013), no. 4, 33–41.
4. J. B. Pendry et al., *Controlling electromagnetic fields*, Science **312** (2006), no. 5781, 1780–1782.
5. N. Yu et al., *Flat optics with designer metasurfaces*, Nat. Mater. **13** (2014), 139–150.
6. N. Meinzer et al., *Plasmonic meta-atoms and metasurfaces*, Nat. Photon. **8** (2014), 889–898.
7. A. I. Kuznetsov et al., *Optically resonant dielectric nanostructures*, Science **354** (2016), no. 6314, aag2472.
8. S. Jahani et al., *All-dielectric metamaterials*, Nat. Nanotechnol. **11** (2016), 23–36.
9. D. R. Smith et al., *Metamaterials and negative refractive index*, Science **305** (2004), no. 5685, 788–792.
10. V. M. Shalaev, *Optical negative-index metamaterials*, Nat. Photon. **1** (2007), 41–48.
11. K. O'Brien et al., *Predicting nonlinear properties of metamaterials from the linear response*, Nat. Mater. **14** (2015), 379–383.
12. G. Li et al., *Continuous control of the nonlinearity phase for harmonic generations*, Nat. Mater. **14** (2015), 607–612.
13. X. Ni et al., *An ultrathin invisibility skin cloak for visible light*, Science **18** (2015), no. 6254, 1310–1314.
14. N. Yu et al., *Light propagation with phase discontinuities: generalized laws of reflection and refraction*, Science **21** (2011), no. 6054, 333–337.
15. D. Lin et al., *Dielectric gradient metasurface optical elements*, Science **345** (2014), 298–302.
16. P. Genevet et al., *Holographic optical metasurfaces: a review of current progress*, Rep. Prog. Phys. **78** (2015), 024401.
17. M. I. Shalaev et al., *High-efficiency all-dielectric metasurfaces for ultracompact beam manipulation in transmission mode*, Nano Lett. **15** (2015), 6261–6266.
18. J. Jin et al., *Nanostructured holograms for broadband manipulation of vector beams*, Nano Lett. **13** (2013), 4269–4274.

19. P. Genevet et al., *Recent advances in planar optics: from plasmonic to dielectric metasurfaces*, Optica **4** (2017), no. 1, 139e152.
20. H.-H. Hsiao et al., *Fundamentals and applications of metasurfaces*, Small Methods **1** (2017), 1600064.
21. L. Huang et al., *Metasurface holography: from fundamentals to applications*, Nanophoton. **7** (2018), no. 6, 1169–1190.
22. L. Huang et al., *Dispersionless phase discontinuities for controlling light propagation*, Nano Lett. **12** (2012), no. 11, 5750–5755.
23. A. Arbabi et al., *Subwavelength-thick lenses with high numerical apertures and large efficiency based on high-contrast transmit arrays*, Nat. Commun. **6** (2015), 7069.
24. M. Decker et al., *High-efficiency dielectric Huygens' surfaces*, Adv. Opt. Mater. **3** (2015), 813–820.
25. K. E. Chong et al., *Efficient polarization-insensitive complex wavefront control using Huygens' metasurfaces based on dielectric resonant meta-atoms*, ACS Photon. **3** (2016), no. 4, 514–519.
26. X. Ni et al., *Metasurface holograms for visible light*, Nat. Commun. **4** (2015), 2807.
27. L. Huang et al., *Three-dimensional optical holography using a plasmonic metasurface*, Nat. Commun. **4** (2013), 2808.
28. G. Zheng et al., *Metasurface holograms reaching 80% efficiency*, Nat. Nanotechnol. **10** (2015), 308–312.
29. M. Khorasaninejad et al., *Metalenses at visible wavelengths: diffraction-limited focusing and subwavelength resolution imaging*, Science **352** (2016), no. 6290, 1190–1194.
30. B. H. Chen et al., *GaN metalens for pixel-level full-color routing at visible light*, Nano Lett. **17** (2017), no. 10, 6345–6352.
31. E. Arbabi et al., *MEMS-tunable dielectric metasurface lens*, Nat. Commun. **9** (2018), 812.
32. L. Liu et al., *Broadband metasurfaces with simultaneous control of phase and amplitude*, Adv. Mater. **26** (2014), 5031–5036.
33. E.-Y. Song et al., *Compact generation of airy beams with C-aperture metasurface*, Adv. Opt. Mater. **5** (2017), 1601028.
34. G.-Y. Lee et al., *Complete amplitude and phase control of light using broadband holographic metasurfaces*, Nanoscale **10** (2018), 4237–4245.
35. Y.-W. Huang et al., *Aluminum plasmonic multicolor meta-hologram*, Nano Lett. **15** (2015), no. 5, 3122–3127.
36. W. Wan et al., *Full-color plasmonic metasurface holograms*, ACS Nano **10** (2016), no. 12, 10671–10680.
37. X. Li et al., *Multicolor 3D meta-holography by broadband plasmonic modulation*, Sci. Adv. **2** (2016), e1601102.
38. B. Wang et al., *Visible-frequency dielectric metasurfaces for multiwavelength achromatic and highly dispersive holograms*, Nano Lett. **16** (2016), no. 8, 5235–5240.
39. W. T. Chen et al., *High-efficiency broadband meta-hologram with polarization-controlled dual images*, Nano Lett. **14** (2013), 225–230.
40. A. Arbabi et al., *Dielectric metasurfaces for complete control of phase and polarization with subwavelength spatial resolution and high transmission*, Nat. Nanotechnol. **10** (2015), 937–943.
41. J. P. B. Mueller et al., *Metasurface polarization optics: independent phase control of arbitrary orthogonal states of polarization*, Phys. Rev. Lett. **118** (2017), no. 5, 113901.
42. M. Khorasaninejad et al., *Broadband and chiral binary dielectric meta-holograms*, Sci. Adv. **13** (2016), no. 5, e1501258.
43. D. Wen et al., *Helicity multiplexed broadband metasurface holograms*, Nat. Commun. **6** (2015), 8241.
44. W. Ye et al., *Spin and wavelength multiplexed nonlinear metasurface holography*, Nat. Commun. **7** (2016), 11930.
45. L. Li et al., *Electromagnetic reprogrammable coding-metasurface holograms*, Nat. Commun. **8** (2017), 197.
46. S.-Y. Lee et al., *Holographic image generation with a thin-film resonance caused by chalcogenide phase-change material*, Sci. Rep. **7** (2017), 41152.
47. Q. Wang et al., *Optically reconfigurable metasurfaces and photonic devices based on phase change materials*, Nat. Photon. **10** (2015), 60–65.
48. X. Yin et al., *Beam switching and bifocal zoom lensing using active plasmonic metasurfaces*, Light Sci. Appl. **6** (2017), e17016.
49. J. Li et al., *Addressable metasurfaces for dynamic holography and optical information encryption*, Sci. Adv. **4** (2018), eaar6768.
50. W. T. Chen et al., *A broadband achromatic metalens for focusing and imaging in the visible*, Nat. Nanotechnol. **13** (2018), 220–226.
51. S. Wang et al., *A broadband chromatic metalens in the visible*, Nat. Nanotechnol. **13** (2018), 227–232.
52. E. Arbabi et al., *Two-photon microscopy with a double-wavelength metasurface objective lens*, Nano Lett. **18** (2018), 4943–4948.
53. A. Arbabi et al., *Miniature optical planar camera based on a wide-angle metasurface doublet corrected for monochromatic aberrations*, Nat. Commun. **7** (2016), 13682.
54. M. Faraji-Dana et al., *Compact folded metasurface spectrometer*, Nat. Commun. **9** (2018), 4196.
55. H. Pahlevaninezhad et al., *Nano-optic endoscope for high-resolution optical coherence tomography in vivo*, Nat. Photon. **12** (2018), 540–547.
56. R. Zhao et al., *Multichannel vectorial holographic display and encryption*, Light Sci. Appl. **7** (2018), 95.
57. G.-Y. Lee et al., *Metasurface eyepiece for augmented reality*, Nat. Commun. **9** (2018), 4562.

AUTHOR BIOGRAPHIES

Gun-Yeal Lee received his BS degrees in Electrical and Computer Engineering and Physics from Seoul National University, Seoul, Korea in 2015. He is currently pursuing the PhD degree in Electrical and Computer Engineering from Seoul National University, Rep. of Korea. His main research interests include nanophotonics, optical engineering, optical metamaterials and metasurfaces.

Jangwoon Sung received his BS degree in Electrical Engineering from the School of Electrical Engineering and Computer Science, Seoul National University, Rep. of Korea, in 2016, where he is currently pursuing the PhD degree. His main research interests include nanoelectromagenetism, plasmonics, metamaterials and metasurfaces.

Byoungho Lee received his PhD degree from University of California at Berkeley in Electrical Engineering and Computer Science in 1993. Since September 1994, he has been with the School of Electrical and Computer Engineering, Seoul National University, Rep. of Korea where he is now serving as the Head. Prof. Lee is a Fellow of SPIE, OSA and IEEE, and a Member of the Korean Academy of Science and Technology and Senior Member of the National Academy of Engineering of Korea. He received several awards including National Science Badge of Jinbojang. He has served on the Board of Directors of OSA. Prof. Lee is the President-Elect of the Optical Society of Korea and is on the editorial board of Advances in *Optics* and *Photonics* and *Light: Science and Applications*. His current research interests include 3D imaging, digital holography, augmented/virtual reality, metasurfaces and nanophotonics.